

## Trajectory tracking for non-Markovian quantum systems

S. L. Wu and W. Ma\*

*School of Physics and Materials Engineering, Dalian Nationalities University, Dalian 116600, China*

(Received 15 September 2021; accepted 16 December 2021; published 3 January 2022)

We propose a systematic scheme to engineer quantum states of a quantum system governed by a time-convolutionless non-Markovian master equation. According to the idea of reverse engineering, the general algebraic equation to determine the control parameters, such as coherent and incoherent control fields, is presented. Without artificially engineering the time-dependent decay rates and retaining the environment-induced Lamb shifts, the quantum state can still be transferred into the target state in a finite period of time along an arbitrary designed trajectory strictly in Hilbert space. As an application, we apply our scheme to a driven two-level non-Markovian system and realize instantaneous-steady-state tracking and a complete population inversion with control parameters which are available in experimental settings.

DOI: [10.1103/PhysRevA.105.012204](https://doi.org/10.1103/PhysRevA.105.012204)

### I. INTRODUCTION

Driving quantum systems, especially open quantum systems, to desired target states with very high fidelity is a central goal in quantum sciences and technologies to realize efficient and scalable devices beyond the current state of proof-of-principle demonstrations [1–3]. To control open quantum systems with Markovian dynamics, many innovative schemes have been proposed, such as the adiabatic steady-state scheme [4], the shortcut-to-equilibration scheme [5], the dissipative steady-state-preparation scheme [6,7], and the mixed-state inverse-engineering scheme [8]. These schemes transfer the quantum state into the target steady state with a satisfactory fidelity.

But engineering a quantum state of the non-Markovian quantum system is a different matter. Due to the memory effects of the environment, the next state of a non-Markovian quantum system is determined by each of its previous states [9]. The decay rates are time dependent and may temporarily acquire negative values [10]. This negative decay rate pushes the information (coherence and/or energy) to flow back into the open quantum system after the information dissipates into the environment [11]. Therefore, driving the non-Markovian quantum systems into a desired target state along an exact and designable trajectory definitely is a nontrivial task.

In this paper, we focus on this issue and propose a control scheme for non-Markovian quantum systems, which are governed by the time-convolutionless master equation [12]. By parametrizing the trajectory of the quantum state from the initial state to the target state, the control parameters can be determined by reverse engineering time-dependent control Liouvillians. In this way, the quantum state of the non-Markovian quantum system is transferred into the target state strictly along the parameterized trajectory. It should be emphasized that, since the spectrum density of the environment is difficult to engineer in the experiments [13], we do not select

the decay rates as a means of incoherent control. Although the time-dependent decay rates draw the quantum state out of the trajectory, our scheme can eliminate this effect and keep the quantum state on the designed trajectory. We examine our scheme by applying it to quantum state engineering tasks of a driven two-level non-Markovian system. Instantaneous steady-state tracking and complete population inversion are realized. In this scenario, two-level non-Markovian systems are not only kinematically controllable but also dynamically controllable, which is impracticable for the Markovian case.

This paper is organized as follows. In Sec. II, we present the exact trajectory-control scheme for non-Markovian quantum systems governed by the time-convolutionless master equation. Taking a non-Markovian two-level system as an example, instantaneous-steady-state tracking and population inversion are considered in Sec. III. We show that, attributed to information backflows, the population can be completely transferred into the excited state of the two-level system with the available control parameters in experiments. Finally, we give conclusions and a discussion in Sec. IV.

### II. METHOD

In this work, we consider open quantum systems, where the coupling to a reservoir leads to a non-Markovian dynamics for the system density matrix  $\rho(t)$ , described by a time-convolutionless master equation in the Lindblad form,

$$\begin{aligned} \partial_t \rho(t) &= \hat{\mathcal{L}}[\rho] \\ &= -i[H(t), \rho] + \sum_{\alpha} \gamma_{\alpha}(t) \mathcal{D}[L_{\alpha}](\rho), \end{aligned} \quad (1)$$

where  $H(t)$  is the Hamiltonian containing the coherent controls on the system and the Lamb shifts induced by the coupling to the reservoir and  $\mathcal{D}[L_{\alpha}]$  is the Lindbladian with a Lindblad operator  $L_{\alpha}$ ,

$$\mathcal{D}[L_{\alpha}](\rho) = 2L_{\alpha}(t)\rho L_{\alpha}^{\dagger}(t) - \{L_{\alpha}^{\dagger}(t)L_{\alpha}(t), \rho\}. \quad (2)$$

Each Lindblad operator  $L_{\alpha}(t)$  is associated with a dissipation channel occurring at the time-dependent rate  $\gamma_{\alpha}(t)$ . We

\*mawei@dlnu.edu.cn

consider the case where  $H(t)$ ,  $\gamma_\alpha(t)$ , and  $L_\alpha(t)$  are time dependent. This kind of master equation can be applied, for example, to photonic quantum systems [14] and mesoscopic electron-phonon systems [15].

Since the time-convolutionless master equation is linear in  $\rho(t)$ , it is convenient to describe this master equation as a superoperator formalism in Hilbert-Schmidt space [16], wherein the density matrix is represented by an  $N^2$ -dimensional vector,

$$|\rho(t)\rangle\rangle = (\rho_0(t), \rho_1(t), \dots, \rho_{N^2-1}(t))^\dagger, \quad (3)$$

where  $\rho_i(t)$  is the  $i$ th component of  $|\rho(t)\rangle\rangle$  with a time-independent basis  $B_i$  of the Hilbert-Schmidt space satisfying  $\rho_i(t) = \text{Tr}[\rho(t)B_i]$ . On the other hand, the Liouvillian superoperator becomes an  $N^2 \times N^2$  time-dependent supermatrix  $\mathcal{L}(t)$  whose elements are given by  $\mathcal{L}_{ij}(t) = \text{Tr}\{B_i^\dagger(\hat{\mathcal{L}}[B_j])\}$ . Then the master equation as shown in Eq. (1) reads

$$\partial_t |\rho(t)\rangle\rangle = \mathcal{L}(t)|\rho(t)\rangle\rangle, \quad (4)$$

with the Liouvillian supermatrix

$$\begin{aligned} \mathcal{L}(t) = & -i[H \otimes I - I \otimes H^T] \\ & + \sum_{\alpha} \gamma_{\alpha} (2L_{\alpha} \otimes L_{\alpha}^* - L_{\alpha}^{\dagger} L_{\alpha} \otimes I - I \otimes L_{\alpha}^T L_{\alpha}^*), \end{aligned} \quad (5)$$

where  $A^T$  denotes the transposition of the operator  $A$  and  $I$  is the identity operator.

The aim of the control scheme is to transfer the quantum system from a known and arbitrary initial state  $\rho(0)$  to a desired target state  $\rho(t_f)$  along a preset trajectory. The choice of the bases of the Hilbert-Schmidt is not unique, and the principle of this choice is determined by how we simplify complexity to obtain feasible control parameters in the Liouvillian superoperator. Without the loss of generality, the basis set of the Hilbert-Schmidt space can be chosen to be the  $SU(N)$  Hermitian generators  $\{T_i\}_{i=1}^{N^2-1}$  and the identity operator  $T_0 \equiv I$ . Thus, the density matrix can be expanded by these bases and yields

$$|\rho(t)\rangle\rangle = \frac{1}{N} \left( |I\rangle\rangle + \sqrt{\frac{N(N-1)}{2}} \sum_{i=1}^{N^2-1} r_i |T_i\rangle\rangle \right), \quad (6)$$

where  $\vec{r} = (r_1, r_2, \dots, r_{N^2-1})$  is the generalized Bloch vector with  $\sum_i |r_i|^2 < 1$ . Within this notation, the density matrix can be parameterized by  $N^2 - 1$  independent coefficients.

On the other hand, the Liouvillian superoperator contains all of the control parameters which can be applied in a real-world experimental setting. The control on the quantum system comes from two types, i.e., the coherent control and the incoherent control. The coherent controls on the quantum system applied in the experiment are contained in the Hamiltonian of the Liouvillian superoperator. By using the  $SU(N)$  Hermitian generators  $\{T_i\}_{i=0}^{N^2-1}$  ( $T_0 \equiv I$  is the identity operator), the Hamiltonian can be expressed as

$$H(t) = \sum_{i=0}^{N^2-1} c_i(t) T_i, \quad (7)$$

where  $c_i(t)$  denotes the control parameter for the coherent operation  $T_i$  on the system. The incoherent controls come from the couplings to the environment, which are reflected in the

master equation by the Lindbladian. Generally, the Lindblad operators can be written as superpositions of the  $SU(N)$  Hermitian generators, such as

$$L_{\alpha}(t) = \sum_{j=1}^{N^2-1} l_j^{(\alpha)}(t) T_j, \quad (8)$$

with complex expansion coefficients  $l_j^{(\alpha)}(t)$ . Here we assume that these complex coefficients  $\{l_j^{(\alpha)}(t)\}$  include incoherent control parameters which are tunable in experiment and influence the system in incoherent ways. These incoherent control parameters include, but are not limited to, the main excitation numbers of the environment [17,18], the correlation of the environment [19], and even extra noise [20]. As a restriction on our scheme, the correlation functions of the environment are invariant. Thus, the decay rates and the Lamb shifts caused by the interaction between the open quantum systems and the environments cannot be changed artificially, which distinguishes our scheme from previous schemes on this topic [21].

Here we are in the position to determine all of the control parameters (coherent and incoherent) in reverse. In fact, the density-operator vector is the solution of Eq. (4). Our scheme is to preset the density operator  $\rho(t)$  and then to determine the control parameters  $\{c_i(t), l_j^{(\alpha)}(t)\}$  using Eq. (4). At the beginning, we parametrize the density operator by the generalized Bloch vector as shown in Eq. (6). The initial and final Bloch vectors have to correspond to the initial and target states of the control task. Thus, the time-dependent Bloch vector corresponds to a trajectory of the quantum state in the Hilbert space, which connects the initial state and target state. Then we deal with the Liouvillian supermatrix. The elements of the Liouvillian supermatrix can be determined by  $\mathcal{L}_{ij}(t) = \text{Tr}\{T_i^\dagger(\hat{\mathcal{L}}[T_j])\}$ . In order to distinguish the coherent and incoherent control types, we divide the Liouvillian supermatrix into three parts. Thus, we rewrite the time-convolutionless master equation in components of the generalized Bloch vector,

$$\partial_t r_i(t) = \sum_{j=1}^{N^2-1} (C_{ij} + \mathcal{I}_{ij}) r_j(t) + \mathcal{L}_i^0. \quad (9)$$

The coherent part reads

$$C_{ij} = \sum_{k=1}^{N^2-1} c_k(t) \frac{f_{kji}}{2}, \quad (10)$$

and the incoherent part takes the form

$$\mathcal{I}_{ij} = \sum_{m,n=0}^{N^2-1} \left( \sum_{\alpha} \gamma_{\alpha} l_m^{(\alpha)}(t) l_n^{(\alpha)*}(t) \right) s_{mn,ji}, \quad (11)$$

with

$$\begin{aligned} s_{mn,ji} = & \frac{1}{2N} (\delta_{im} \delta_{jn} - \delta_{mn} \delta_{ij}) \\ & + \frac{1}{4} \sum_{k=1}^{N^2-1} [(i f_{jnk} + d_{jnk})(i f_{imk} + d_{imk}) \\ & - (i f_{mnk} + d_{mnk}) d_{kji}], \end{aligned} \quad (12)$$

where  $f_{ijk}$  and  $d_{ijk}$  are the structure constants and the  $d$  coefficients of the  $SU(N)$  Lie algebra, respectively. Moreover, the last terms in Eq. (9) can be written as

$$\mathcal{L}_k^0 = \sum_{\alpha} \gamma_{\alpha}(t) \left( \sum_{i,j=1}^{N^2-1} l_i^{(\alpha)}(t) l_j^{(\alpha)*}(t) g_{ijk} \right),$$

with  $g_{ijk} = [(i f_{jik} + d_{jik}) - (i f_{ijk} + d_{ijk})]$ . The derivation of the coherent and incoherent parts of the Liouvillian supermatrix can be found in Appendix A.

In fact, Eq. (9) is not only linear to the components of the Bloch vector but also linear to the control parameters  $\{c_i(t), \sum_{\alpha} \gamma_{\alpha} l_i^{(\alpha)}(t) l_j^{(\alpha)*}(t)\}$ . Here, we further assume that there is only one tunable incoherent control parameter in every Lindbladian  $\mathcal{D}[L_{\alpha}]$ , i.e.,  $l_i^{(\alpha)}(t) = \sqrt{\tilde{c}_{\alpha}(t)} \tilde{l}_i^{(\alpha)}$ , where  $\tilde{c}_{\alpha}(t)$  is a real incoherent control parameter and  $\{\tilde{l}_i^{(\alpha)}\}$  are time-independent expansion coefficients. Thus, we have  $\sum_{\alpha} \gamma_{\alpha} l_i^{(\alpha)}(t) l_j^{(\alpha)*}(t) = \sum_{\alpha} \gamma_{\alpha} \tilde{c}_{\alpha}(t) \tilde{l}_i^{(\alpha)} \tilde{l}_j^{(\alpha)*}$ . In this notation, the equations of the control parameters are given by

$$\sum_j \Lambda_{ij}^c c_j + \sum_{\alpha} \gamma_{\alpha} (\Lambda_{\alpha i}^i + \Lambda_{\alpha i}^0) \tilde{c}_{\alpha} - \partial_t r_i(t) = 0 \quad \forall i, \quad (13)$$

where the coefficient matrices for the coherent control and incoherent parameters are

$$\begin{aligned} \Lambda_{ij}^c &= \sum_{k=1}^{N^2-1} r_k(t) \frac{f_{jki}}{2}, \\ \Lambda_{\alpha i}^i &= \sum_{j,m,n=0}^{N^2-1} r_j(t) [\tilde{l}_m^{(\alpha)}(t) \tilde{l}_n^{(\alpha)*}(t)] s_{mn,ji}, \\ \Lambda_{\alpha i}^0 &= \sum_{j,k=1}^{N^2-1} \tilde{l}_j^{(\alpha)}(t) \tilde{l}_k^{(\alpha)*}(t) g_{jki}. \end{aligned} \quad (14)$$

In order to obtain the control parameters  $\{c_i(t), \tilde{c}_{\alpha}(t)\}$ , we need to solve above equations.

As we see, Eq. (13) cannot provide a single unique solution for the control parameters in general. In practice, not all of the control parameters can be applied to the system. For instance, a  $\Delta$ -type coherence control can be realized in an artificial structure but not in real atoms via dipole-dipole coupling due to the selection rule [22]. Also, the decoherence channels used in the scheme are restricted by the real-world setting. In other words, open quantum systems must be dynamically controllable [23,24]. Therefore, for the selection of control parameters in our scheme, two principles have to be met: (i) The number of control parameters is equal to number of equations in Eq. (13), which ensures a single unique control parameter in the control scheme. (ii) All of the control technologies corresponding to the control parameters have to be available in the real-experiment setting. To meet the above requirements, the control technologies with corresponding control parameters have to be selected for not only the experimental conditions in the laboratory but also the symmetry of open quantum systems [25,26].

### III. APPLICATIONS: A TWO-LEVEL NON-MARKOVIAN SYSTEM

We consider a two-level system with transition frequency  $\omega_0$  driven by an external laser of frequency  $\omega_L$  [27,28]. There is a detuning  $\Delta = \omega_0 - \omega_L$  between the two-level system and the external laser. The two-level atom is embedded in a bosonic reservoir at a finite temperature  $T$ . In a rotating frame, the Hamiltonian can be written as

$$H = H_s + H_e + H_i, \quad (15)$$

with

$$\begin{aligned} H_s &= \Delta \sigma_+ \sigma_- + \Omega(t) \sigma_+ + \Omega^*(t) \sigma_-, \\ H_e &= \sum_k \Omega_k a_k^{\dagger} a_k, \\ H_i &= \sum_k g_k \sigma_+ a_k + \text{H.c.}, \end{aligned} \quad (16)$$

where  $\Delta = \omega_0 - \omega_L$ ,  $\Omega_k = \omega_k - \omega_L$ ,  $\sigma_+ = |e\rangle\langle g|$ ,  $\Omega(t) = \Omega_s(t) + i\Omega_y(t)$  is the time-dependent control field, H.c. stands for the Hermitian conjugation, and  $a_k$  and  $g_k$  stand for the annihilation operator and coupling constant, respectively.

Using the atomic coherent-state path-integral method [27], an exact non-Markovian master equation can be obtained to describe the dynamics of the open two-level system,

$$\begin{aligned} \partial_t \rho(t) &= \hat{\mathcal{L}}_0(t) \rho(t) \\ &= -i[H_s^R(t), \rho(t)] + \Gamma_0(N+1) \hat{\mathcal{D}}[\sigma_-][\rho(t)] \\ &\quad + \Gamma_0 N \hat{\mathcal{D}}[\sigma_+][\rho(t)], \end{aligned} \quad (17)$$

with the effective Hamiltonian

$$H_s^R(t) = s_0(t) \sigma_+ \sigma_- + \Omega^R(t) \sigma_+ + \Omega^{R*}(t) \sigma_-. \quad (18)$$

$s_0(t)$  and  $\Omega^R(t)$  are the Lamb shift and the renormalized driving field, respectively, which are results of the memory effects of the bosonic reservoir. The time-dependent decay rate  $\Gamma_0(t)$  describes the dissipative non-Markovian dynamics due to the interaction between the system and environment.  $N = [\exp(\hbar\omega_0/kT_0) - 1]^{-1}$  stands for the mean excitation number. The decay rate  $\Gamma_0$  and the main excitation number  $N$  are both associated with the spectral density and the temperature  $T_0$  of the reservoir. These time-dependent coefficients are given explicitly as follows:

$$s_0(t) = -\text{Im} \left[ \frac{\partial_t u(t)}{u(t)} \right], \quad \Gamma_0(t) = -\text{Re} \left[ \frac{\partial_t u(t)}{u(t)} \right], \quad (19)$$

$$\Omega^R(t) = i \left[ \partial_t h(t) - h(t) \frac{\partial_t u(t)}{u(t)} \right], \quad (20)$$

where  $\text{Re}[\cdot]$  and  $\text{Im}[\cdot]$  represent the real and imaginary parts of the argument, respectively.  $u(t)$  and  $h(t)$  satisfy the following equations:

$$\partial_t u(t) + i\Delta u(t) + \int_0^t f(t-t') u(t') dt' = 0, \quad (21)$$

$$\partial_t h(t) + i\Delta h(t) + \int_0^t f(t-t') h(t') dt' = -i\Omega, \quad (22)$$

with

$$f(t-t') = \int d\omega J(\omega) \exp[-i(\omega - \omega_L)(t-t')], \quad (23)$$

and the boundary conditions  $u(0) = 1$  and  $h(0) = 0$ . We assume that the spectral density of the bosonic reservoir has a Lorentzian form [27,29,30]:

$$J(\omega) = \frac{\gamma_0}{2\pi} \frac{\lambda^2}{(\omega - \omega_0 + \delta)^2 + \lambda^2}, \quad (24)$$

where  $\delta = \omega_0 - \omega_c$  is the detuning of  $\omega_c$  to  $\omega_0$ ,  $\omega_c$  is the center frequency of the cavity, and  $\lambda$  is the spectral width of the reservoir. The parameter  $\gamma_0$  is the decoherence strength of the system in the Markovian limit with a flat spectrum. Substituting Eq. (24) into Eq. (23), we obtain the two-time correlation functions:

$$f(t - t') = \frac{1}{2} \lambda \Gamma \exp[-(\lambda + i\Delta - i\delta)(t - t')]. \quad (25)$$

Thus, the solutions of Eqs. (21) and (22) take the forms

$$u(t) = k(t) \left[ \cosh\left(\frac{dt}{2}\right) + \frac{\lambda + i\delta}{d} \sinh\left(\frac{dt}{2}\right) \right], \quad (26)$$

$$h(t) = -i \int_0^t \Omega(t') u(t - t') dt', \quad (27)$$

where  $k(t) = \exp[-(\lambda + 2i\Delta - i\delta)t/2]$  and  $d = \sqrt{(\lambda - i\delta)^2 - 2\gamma_0\lambda}$ .

To reverse engineer the non-Markovian two-level system, we parametrize the quantum state by a Bloch vector, which can be written as

$$|\varrho(t)\rangle\rangle = \frac{1}{2} \left( |I\rangle\rangle + \sum_{i=x,y,z} r_i |\sigma_i\rangle\rangle \right), \quad (28)$$

where  $r_i$  is the  $i$ th component of the Bloch vectors and  $\sigma_i$  is the  $i$ th component of the Pauli operators. Thus, the quantum state of the two-level system has three independent parameters. The effective Hamiltonian can be rewritten as

$$H_s^R(t) = s_0(t) \sigma_+ \sigma_- + \Omega_x^R(t) \sigma_x + \Omega_y^R(t) \sigma_y. \quad (29)$$

We have assumed that the spectrum density is untunable in experimental settings, so the decay rate  $\Gamma_0(t)$  cannot be a candidate for the incoherent control parameters. Therefore, the coherent control parameters are chosen to be  $\Omega_x^R(t)$  and  $\Omega_y^R(t)$ , while the main excited number  $N(t)$  acts as the incoherent control parameter. Inserting the control parameters and the components of the Bloch vector into Eq. (9) yields

$$\begin{aligned} \dot{r}_x &= 2\Omega_y^R r_z - s_0 r_y - (2N + 1)\Gamma_0 r_x, \\ \dot{r}_y &= s_0 r_x - 2\Omega_x^R r_z - (2N + 1)\Gamma_0 r_y, \\ \dot{r}_z &= 2\Omega_x^R r_y - 2\Omega_y^R r_x - 2\Gamma_0[(2N + 1)r_z + 1], \end{aligned} \quad (30)$$

where  $\dot{r}_i$  denotes the time derivative of the  $i$ th component of the Bloch vector. For the sake of brevity, we also ignored “ $(t)$ .” The goal of the reverse-engineering scheme is to find the control parameters which drive the two-level system to evolve as users prescribe. To achieve this goal, we reverse

solve Eq. (30) and obtain

$$\begin{aligned} \Omega_x^R &= \frac{(r^2 + r_z^2)(r_x s_0 - \dot{r}_y) + (\vec{r} \cdot \dot{\vec{r}} + 2\Gamma_0 r_z) r_y}{2r_z(r^2 + r_z^2)}, \\ \Omega_y^R &= \frac{(r^2 + r_z^2)(r_y s_0 + \dot{r}_x) - (\vec{r} \cdot \dot{\vec{r}} + 2\Gamma_0 r_z) r_x}{2r_z(r_x^2 + r_y^2 + 2r_z^2)}, \\ N &= -\frac{2\Gamma_0 r_z + \vec{r} \cdot \dot{\vec{r}} + \Gamma_0(r^2 + r_z^2)}{2\Gamma_0(r^2 + r_z^2)}, \end{aligned} \quad (31)$$

with  $r^2 = r_x^2 + r_y^2 + r_z^2$  and  $\vec{r} \cdot \dot{\vec{r}} = r_x \dot{r}_x + r_y \dot{r}_y + r_z \dot{r}_z$ .

In the case of Markovian dynamics, the Lamb shift vanishes ( $s_0 = 0$ ), and the decay rate is time independent ( $\Gamma_0 = \gamma_0$ ).  $\Omega_{x,y}^R$  are the control fields acting on the two-level system. Therefore, the set of control parameters proposed in Eq. (31) is a control protocol for two-level systems in a Markovian environment. In other words, our scheme is also an available option for controlling Markovian quantum systems. We can rewrite the last equation in Eq. (31) as  $2\Gamma_0 r_z + \vec{r} \cdot \dot{\vec{r}} = -(2N + 1)(r^2 + r_z^2)\Gamma_0$ . By substituting this equation into the expression for  $\Omega_{x,y}^R$ , we obtain the same control field as that used in Ref. [31]. Moreover, we may set the main excitation number  $N$  as invariant in the control process, which is the very constraint condition mentioned in Ref. [31].

Here we want to emphasize that the control parameters presented in Eq. (31) is not the only choice to reverse engineer the non-Markovian two-level system. For instance, while we keep the incoherent control protocol invariant, the detuning  $\Delta$  can also be selected as a coherent control parameter, which will provide another control protocol without using the control parameter  $\Omega_y^R$  (see Appendix B). In fact, whether coherent or incoherent, as long as the solutions of Eq. (13) exist, these control parameters can be candidates for control protocols. This means that the two-level system is kinematically controllable for our control scheme [23,32]. If the control protocol is totally coherent, it can be verified that Eq. (13) has no solution, which indicates that open two-level systems are kinematically incompletely controllable in the pure coherent control protocol [23,33]. On the other hand, there are always restrictions on controls, such as the finite pulse strength and detuning and non-negative main excitation numbers. Thus, although the system is kinematically controllable with the proper control protocol, it still cannot be realized in the real experimental setting. In other words, an open quantum system which is kinematically controllable is not always dynamically controllable using the available set of controls [33]. As shown in Eq. (31), the control parameters are related to the trajectory of the quantum state in the Hilbert space (components of the Bloch vector). Therefore, our scheme can enhance the dynamical controllability by designing proper trajectories of the quantum states in the Hilbert space.

### A. Steady-state tracking

In this section, we drive the two-level non-Markovian system to track the instantaneous steady state of a particular reference Liouvillian  $\mathcal{L}_0(t)$  [34], which is often used in quantum thermodynamics [35,36] and the quantum many-body theory [4]. In particular, transferring the quantum state of open quantum systems strictly along the instantaneous steady state

is critical for optimizing the performance of the quantum heat engine [37,38].

Let the reference Liouvillian  $\hat{\mathcal{L}}_0(t)$  take the same form as the non-Markovian master equation presented in Eq. (17) with the reference Hamiltonian

$$H_0(t) = s_0(t)\sigma_+\sigma_- + \Omega_0^R(t)\sigma_x$$

and a constant main excitation number  $N_0$ . Thus, the reference Liouvillian supermatrix reads

$$\mathcal{L}_0(t) = \Gamma_0 \begin{pmatrix} -(N'+1) & i\frac{\Omega_0^R}{\Gamma_0} & -i\frac{\Omega_0^R}{\Gamma_0} & N'-1 \\ i\frac{\Omega_0^R}{\Gamma_0} & -N' - i\frac{s_0}{\Gamma_0} & 0 & -i\frac{\Omega_0^R}{\Gamma_0} \\ -i\frac{\Omega_0^R}{\Gamma_0} & 0 & -N' + i\frac{s_0}{\Gamma_0} & i\frac{\Omega_0^R}{\Gamma_0} \\ (N'+1) & -i\frac{\Omega_0^R}{\Gamma_0} & i\frac{\Omega_0^R}{\Gamma_0} & -N'+1 \end{pmatrix},$$

with  $N' = 2N_0 + 1$ . The instantaneous steady state of the two-level system is given by the condition  $\mathcal{L}_0(t)|\rho_0(t)\rangle\rangle = 0$ , which yields

$$|\rho_0\rangle\rangle = \frac{1}{z} \begin{pmatrix} N_0(N'^2\Gamma_0^2 + s_0^2) + N'\Omega_0^{R2} \\ (iN'\Gamma_0 - s_0)\Omega_0^R \\ -(iN'\Gamma_0 + s_0)\Omega_0^R \\ (N_0 + 1)(N'^2\Gamma_0^2 + s_0^2) + N'\Omega_0^{R2} \end{pmatrix}, \quad (32)$$

with the factor  $z = N'(\Gamma_0^2 N'^2 + s_0^2 + 2\Omega_x^{R2})$ .

We impose that the initial and final Bloch vectors are the very Bloch vectors for the instantaneous steady state  $|\rho_0(t)\rangle\rangle$  [Eq. (32)] at  $t = 0$  and  $t = t_f$ . Since there is not an adiabatic theorem for the non-Markovian case, the reference Liouvillian  $\hat{\mathcal{L}}_0(t)$  cannot drive the quantum system into the final steady state along the instantaneous steady state, even if  $\dot{\Omega}_0^R \rightarrow 0$ . Hence, it is not necessary to compel  $\Omega_x^R(t) = \Omega_0^R(t)$  at the initial and final moments. What we need to be concerned with is finding a set of proper control parameters which ensures that the quantum state strictly tracks the instantaneous-steady-state trajectory. The instantaneous steady state (32) can be rewritten in the form of the Bloch vector as

$$\begin{aligned} r_x(t) &= -\frac{2}{z} \Omega_0^R(t)s_0(t), \\ r_y(t) &= -\frac{2}{z} N'\Omega_0^R(t)\Gamma_0(t), \\ r_z(t) &= -\frac{1}{z} [s_0(t)^2 + N'^2\Gamma_0(t)^2]. \end{aligned} \quad (33)$$

We suppose that the reference control field  $\Omega_0^R(t)$  tunes up from zero to a finite strength  $\Omega_c$ , and the time derivative of  $\Omega_0^R(t)$  is zero at the initial and final instants. Therefore, we assume the following time-dependent profile of  $\Omega_0^R(t)$ :

$$\Omega_0^R(t) = 6\Omega_c \frac{t^2}{t_f^2} \left( \frac{1}{2} - \frac{t}{3t_f} \right). \quad (34)$$

Substituting Eqs. (19) and (34) into Eq. (31), we can obtain all the analytical expressions for the control parameters, which can drive the quantum state into the target steady state strictly along the instantaneous steady state.

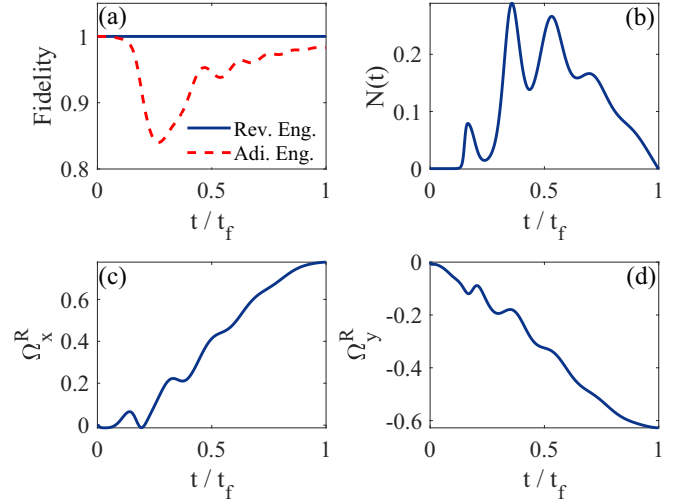


FIG. 1. (a) The fidelity of the reverse-engineering protocol (blue solid line) and the adiabatic-engineering protocol (red dashed line) vs the dimensionless time  $t/t_f$ . The control parameters [(b) the main excitation number  $N$ , (c) the coherent control field  $\Omega_x^R$ , and (d) the coherent control field  $\Omega_y^R$ ] as a function of the dimensionless time  $t/t_f$ . Parameters are  $\lambda = 0.5\gamma_0$ ,  $\Delta = 0.1\gamma_0$ ,  $\delta = 0.5\gamma_0$ ,  $\Omega_c = 10\gamma_0$ ,  $t_f = 10/\gamma_0$ , and  $N_0 = 10^{-5}$ . We set  $\gamma_0 = 1$  as the units of  $\Omega_x^R$  and  $\Omega_y^R$ .

Figure 1(a) shows the evolutions of the fidelities between the quantum state governed by the master equation (17) and the instantaneous steady state given by Eq. (32) plotted for the inverse-engineering protocol (blue solid line) and the adiabatic-engineering protocol (red dashed line). For the reverse-engineering scheme, the quantum state of the open two-level system strictly follows the instantaneous steady state. When the adiabatic-engineering protocol is used, i.e.,  $\Omega_x^R = \Omega_0^R$  and  $\Omega_y^R = 0$ , the fidelity obviously decreases. Even if the performance of the adiabatic-engineering protocol is satisfactory in the long time limit, the quantum state deviates from the steady-state trajectory at the intermediate time due to the rapid oscillation of the decay rate  $\Gamma_0(t)$  and the Lamb shift  $s_0(t)$ .

The main excitation number  $N(t)$  and the control field  $\Omega_{x,y}^R(t)$  are plotted in Figs. 1(b)–1(d). On the one hand, all of the control parameters oscillate with time, which is essential to offset the effect of the rapid oscillation of the decay rate  $\Gamma_0(t)$  and the Lamb shift  $s_0(t)$ . In this way, the quantum state is suppressed in the instantaneous steady state. On the other hand, due to the nonzero Lamb shift  $s_0(t)$ , the coherent control field  $\Omega_y^R(t)$  is needed in the reverse-engineering protocol, which does not appear in the reference Hamiltonian (or Liouvillian). If  $s_0(t) = 0$ , the  $x$ th component of the Bloch vector will be zero, which will result in the absence of the coherent control field  $\Omega_y^R(t)$  [see Eqs. (31) and (33)]. This is the significant difference from the Markovian counterpart of the reverse-engineering protocol.

## B. Population inversion

Similar ideas can be applied to the population inversion of the two-level open quantum state. For convenience, we express the Bloch vector  $\vec{r}$  by means of spherical polar

coordinates, i.e.,

$$r_x = r \sin \theta \sin \phi, \quad r_y = r \cos \theta \sin \phi, \quad r_z = r \cos \phi. \quad (35)$$

Our aim is to transfer the quantum state from the ground state  $|0\rangle$  to the excited state  $|1\rangle$ . Here  $|0\rangle$  and  $|1\rangle$  are the eigenvectors of  $\sigma_z$ . Hence, we set the boundary conditions of the quantum state as  $\phi(0) = \pi$ ,  $r(0) = 1$ ,  $\phi(t_f) = 0$ , and  $r(t_f) = 1$ . It is free to choose the values of  $\theta(0)$  and  $\theta(t_f)$ . According to Eq. (31), when  $\phi \rightarrow \pi/2$ , the coherent control fields  $\Omega_x^R$  and  $\Omega_y^R$  tend to be infinite. In order to eliminate this singularity, we require  $s_0 = 0$ ,  $\dot{s} = 0$ , and  $\ddot{s} = 0$  for  $\phi = \pi/2$ . Here we should mention that the requirement  $s_0(t_i) = 0$  for some intermediate moment  $t_i$  can be realized by picking a proper detuning  $\Delta$ . In addition, for the non-Markovian dynamics of open quantum systems, the decay rates are negative for some intermediate duration. Thus, the main excitation  $N(t)$  will be infinite at the moment for  $\Gamma_0 = 0$ . Yet if we require  $\vec{r} \cdot \dot{\vec{r}} = 0$  at this point, a reasonable main excitation number can be obtained [see Eq. (31)].

First, we show that the population inversion with a pure-state trajectory is kinematically controllable but not dynamically controllable. To interpolate at intermediate times, we consider a polynomial ansatz of  $\theta$  and  $\phi$  as a function of time  $t$ ,

$$\begin{aligned} r(t) &= 1, \quad \phi(t) = \pi \frac{t^2}{t_f^2} \left( 3 - 2 \frac{t}{t_f} \right), \\ \theta(t) &= \theta \left( \frac{t_f}{2} \right) \frac{t^2}{t_f^2} \left( 1 - \frac{t}{t_f} \right)^2, \end{aligned} \quad (36)$$

with  $\theta(0) = \theta(t_f) = 0$  and an arbitrary  $\theta(t_f/2)$  at  $t = t_f/2$ . Under this ansatz, for  $t = t_f/2$ , we have  $\phi(t_f/2) = \pi/2$  and  $\dot{\theta}(t_f/2) = 0$ , which result in reasonable coherent control fields in the control period. Figure 2(a) shows the fidelities between the quantum state  $\rho(t)$  and the preset trajectory given by Eq. (35) for the reverse-engineering protocol (the blue solid line) and the inverse-engineering protocol of closed quantum systems. The control parameters are plotted in Figs. 2(b)–2(d). As we see, the reverse-engineering protocol definitely transfers the quantum state from  $|0\rangle$  to  $|1\rangle$ , while the control parameters evolve smoothly. Therefore, the pure-state protocol is kinematically controllable. But as shown in Fig. 2(b), the main excitation number  $N(t)$  is negative, which is not feasible in an experimental setting, so the reverse-engineering protocol is not dynamically controllable for the pure-state trajectory.

Second, we show that the population inversion is dynamically controllable if a mixed-state trajectory of the two-level non-Markovian system is carefully selected. As we see, the dynamical uncontrollability comes from the negative main excitation number. We can rewrite the main excitation number as

$$N(t) = - \left( \frac{1}{2} + \frac{r_z}{r^2 + r_z^2} + \frac{\partial_t r^2}{4\Gamma_0 (r^2 + r_z^2)} \right), \quad (37)$$

with the length of the Bloch vector  $r = \sqrt{r_x^2 + r_y^2 + r_z^2}$ . If the quantum state is pure, then  $\partial_t r^2 = 0$  and  $r = 1$ , which results in a negative main excitation number. The population inversion corresponds to the Bloch vector from  $r_z(t) = -1$  to

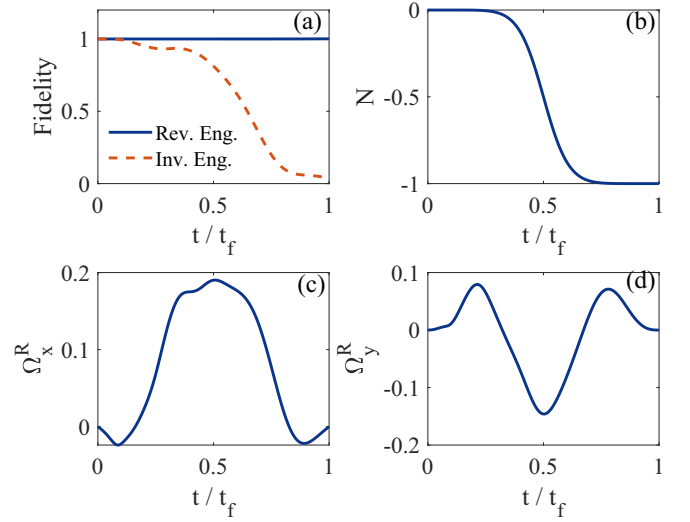


FIG. 2. (a) The evolution of the fidelity of the reverse-engineering protocol (blue solid line) and the adiabatic-engineering protocol (red dashed line). The control parameters [(b) the main excitation number  $N$ , (c) the coherent control field  $\Omega_x^R$ , and (d) the coherent control field  $\Omega_y^R$ ] as a function of the dimensionless time  $t/t_f$ . Parameters are  $\lambda = 0.5\gamma_0$ ,  $\Delta = 0.1\gamma_0$ ,  $\delta = 0.5\gamma_0$ ,  $\Omega_c = 10\gamma_0$ ,  $t_f = 10/\gamma_0$ , and  $N_0 = 10^{-5}$ . We set  $\gamma_0 = 1$  as the units of  $\Omega_x^R$  and  $\Omega_y^R$ .

$r_z(t_f) = 1$ . When  $r_z$  varies from  $-1$  to  $0$ , the second term in Eq. (37) is negative. Moreover, if  $r$  shortens with evolution, the third term in Eq. (37) is also negative. Thus, we can ensure that the main excitation number is always positive in the lower hemisphere of the Bloch sphere. However, in the upper hemisphere of the Bloch sphere, i.e.,  $r_z > 0$ , the second term in Eq. (37) is positive, and  $r$  needs to increase with time, so the main excitation number cannot always be positive in the evolution. However, the decay rate  $\Gamma_0(t)$  is negative at some intermediate moment. Therefore, we propose the following to realize a dynamically controllable population inversion: (i) We set  $t_f$  as the moment where  $\Gamma_0$  reaches the negative maximum for the first time and label  $t_i$  as the moment when  $\Gamma_0(t_i) = 0$  for  $t_i \in (0, t_f)$ , which is illustrated in Fig. 3(a). (ii) Since  $\Gamma_0(t) > 0$  for  $t \in (0, t_i)$ , we impose that  $r_z(t_i) = 0$  and  $r_z(t) < 0$  for  $t < t_i$ . In this way, it is easy to present a positive main excitation number for  $t < t_i$  by selecting a mixed trajectory. (iii) Since  $\Gamma_0(t) < 0$  for  $t \in (t_i, t_f)$ , the third term in Eq. (37) will be negative if  $r^2$  keeps increasing. Thus, it is possible to present a positive main excitation number if  $\vec{r}(t) \cdot \dot{\vec{r}}(t)$  increases fast enough.

As an example, we impose the boundary conditions of the components of the Bloch vector as follows:

$$\begin{aligned} r_y(0) &= 0, & r_y(t_i) &= 0.12, & r_y(t_f) &= 0, \\ \dot{r}_y(0) &= 0, & \dot{r}_y(t_i) &= 0, & \dot{r}_y(t_f) &= 0, \\ r_z(0) &= -1, & r_z(t_i) &= 0, & r_z(t_f) &= 1, \\ \dot{r}_z(0) &= 0, & \dot{r}_z(t_i) &= 0.4, & \dot{r}_z(t_f) &= 1, \end{aligned} \quad (38)$$

and  $r_x(t) = 0$  for all  $t$ . The reason why we selected the boundary conditions in Eq. (38) is to eliminate singular points in the control parameters and obtain a positive main excitation number. As shown in Eq. (31),  $\Omega_x^R$  and  $\Omega_y^R$  have singular

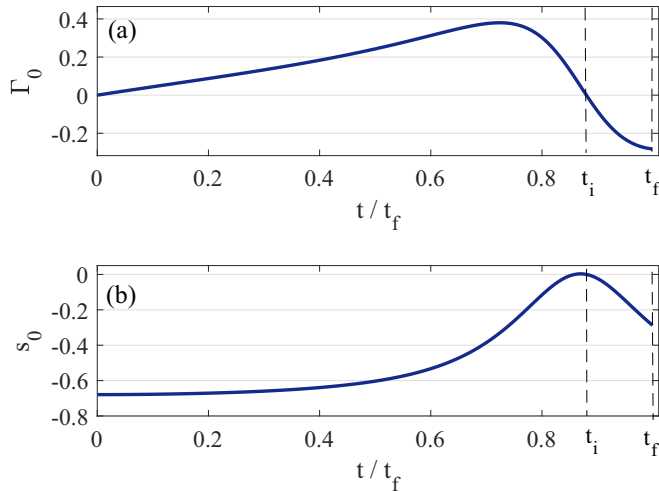


FIG. 3. (a) The decay rate  $\Gamma_0$  and (b) the Lamb shift vs the dimensionless time  $t/t_f$ , where  $t_f$  is the control pulse length and  $t_i$  is the moment where  $r_z = 0$ . Parameters are  $\lambda = 0.1\gamma_0$ ,  $\Delta = -0.6792\gamma_0$ ,  $\delta = 0.1\gamma_0$ ,  $\Omega_c = 1\gamma_0$ , and  $t_f = 9.1201/\gamma_0$ . We set  $\gamma_0 = 1$  as the units of  $\Gamma_0$  and  $s_0$ .

points at  $t = t_i$  because  $r_z(t_i) = 0$ . Thus, we require  $\dot{r}_x(t_i) = \dot{r}_y(t_i) = 0$  and further impose  $s_0(t_i) = 0$ , which is illustrated in Fig. 3(b). On the other hand, if  $\vec{r} \cdot \dot{\vec{r}} > -\Gamma_0 r_z(r_z + 1)$ ,  $N$  will be positive. For  $t = t_i$ , the positive main excitation number requires  $\dot{r}_z(t_i) > -\Gamma_0(t_i)$ . Thus, the time derivative of  $r_z(t_i)$  must be a nonzero and finite positive number. Due to  $r_z(t_i) = \dot{r}_y(t_i) = 0$ , it is not difficult to verify that  $\vec{r} \cdot \dot{\vec{r}} = 0$ , so that the singular point in Eq. (37) is also eliminated. Finally, the time derivative of  $r_z(t_f)$  must be a nonzero and finite positive number, which results in  $N(t_f) > 0$  [see Eq. (37)]. To interpolate at intermediate times, we assume a polynomial ansatz and consider a piecewise interpolation with a time break  $t_i$ . Figure 4(a) shows the numerical results of the quantum state trajectory in the Bloch sphere, which illustrates that the population is transferred from  $|0\rangle$  into  $|1\rangle$  completely. The main excitation number  $N$  and the coherent control fields  $\Omega_x^R$  and  $\Omega_y^R$  are plotted in Figs. 4(b)–4(d), respectively. As shown, the control parameters with the boundary conditions of the trajectory in (38) are reasonable and can be realized in experimental settings. Therefore, the population inversion for the two-level non-Markovian system is definitely dynamically controllable.

#### IV. CONCLUSIONS AND DISCUSSION

In conclusion, based on the idea of reverse engineering, we have proposed a scheme to transfer the quantum state of non-Markovian systems strictly along a designable trajectory in the Hilbert space. For quantum systems governed by a time-convolutionless master equation, we have presented analytical expressions for the control parameters, which are the solution of algebraic equations with quantum state trajectories. Even though the open quantum system suffers from the memory effects of the non-Markovian reservoir (information backflow and/or the Lamb shift), the quantum state can still transfer to the target state strictly along the designed

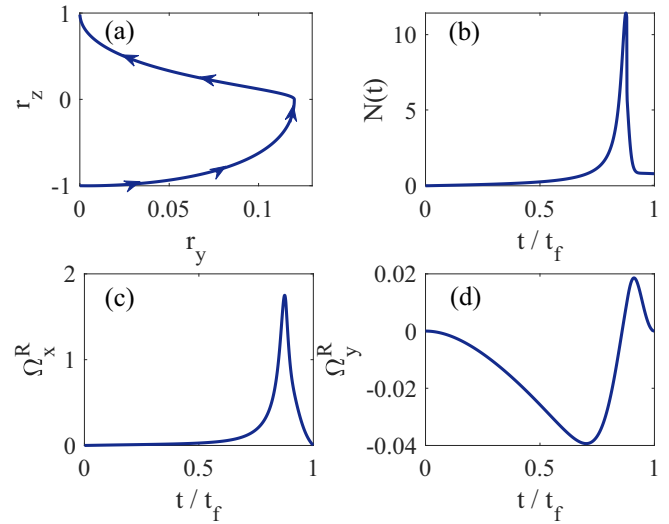


FIG. 4. (a) The evolution of the quantum state trajectory in the Bloch sphere as a function of the dimensionless time  $t/t_f$ . (b) The main excitation number  $N$ , (c) the coherent control field  $\Omega_x^R$ , and (d) the coherent control field  $\Omega_y^R$  as a function of the dimensionless time  $t/t_f$ . Parameters are  $\lambda = 0.1\gamma_0$ ,  $\Delta = -0.6792\gamma_0$ ,  $\delta = 0.1\gamma_0$ ,  $\Omega_c = 1\gamma_0$ , and  $t_f = 9.1201/\gamma_0$ . We set  $\gamma_0 = 1$  as the units of  $\Omega_x^R$  and  $\Omega_y^R$ .

trajectory. Taking the driven non-Markovian two-level system as an example, we presented a concrete control protocol for both instantaneous-steady-state tracking and population inversion. By elaborately designing the trajectory of the quantum state, we showed that the non-Markovian two-level system is not only kinematically controllable but also dynamically controllable. Since the scheme allows us to maintain system coherence and populations in the presence of noise, it may naturally find applications in quantum computing and quantum memory [39,40]. Our scheme can also be applied to numerous quantum control problems, such as quantum state preparation [41], quantum measurement [42], and quantum metrology.

It is meaningful to compare our scheme with the reverse-engineering scheme of Markovian quantum systems [31,43]. For the Markovian dynamics, the quantum system is not dynamically controllable [23,33]. For instance, the complete population inversion of two-level systems cannot be realized in the experimental setting. The population of the excited state is only asymptotically getting closer to 1, which was discussed for the example of the population inversion [31]. Due to the information which can flow back into the open two-level system [44,45], the complete population inversion for the non-Markovian dynamics can be realized by carefully designing the trajectory of the quantum state sweeping in the Hilbert space. In other words, the non-Markovianity will benefit the quantum control process.

#### ACKNOWLEDGMENT

This work is supported by the National Natural Science Foundation of China (NSFC) under Grants No. 12075050 and No. 11775048.

**APPENDIX A: DERIVATION OF EQUATION (9)**

We begin with the time-convolutionless master equation in the superoperator form (4). Inserting the density-operator vector (6) into Eq. (4) [46] yields

$$\partial_t r_i(t) = \sum_{j=1}^{N^2-1} \mathcal{L}_{ij} r_j + \mathcal{L}_i^0, \quad (\text{A1})$$

where the Liouvillian superoperator can be written in the supermatrix form,

$$\hat{\mathcal{L}} = \sum_{ij=1}^{N^2-1} \mathcal{L}_{i,j} |T_i\rangle\rangle\langle\langle T_j| + \sum_{i=1}^{N^2-1} \mathcal{L}_i^0 |T_i\rangle\rangle\langle\langle T_0|, \quad (\text{A2})$$

with  $\mathcal{L}_{ij}(t) = \text{Tr}\{T_i^\dagger(\hat{\mathcal{L}}[T_j])\}$  and  $\mathcal{L}_i^0(t) = \text{Tr}\{T_i^\dagger(\hat{\mathcal{L}}[T_0])\}$ . Here the relation  $\hat{\mathcal{L}}^\dagger(t)|T_0\rangle\rangle = \langle\langle T_0|\hat{\mathcal{L}}(t) = 0$  has been used. We divide the Liouvillian supermatrix into two parts,  $\mathcal{L}_{ij} = \mathcal{C}_{ij} + \mathcal{I}_{ij}$ , where  $\mathcal{I}_{ij}$  ( $\mathcal{C}_{ij}$ ) denotes the incoherent (coherent) part of the Liouvillian supermatrix element  $\mathcal{L}_{ij}$ .

The coherent part comes from the Hamiltonian part in the master equation,

$$\mathcal{C}_{ij} = -i \text{Tr}\{T_i^\dagger [H(t), T_j]\}. \quad (\text{A3})$$

By substituting Eq. (7) into above equation, we have

$$\mathcal{C}_{ij} = -i \sum_{k=0}^{N^2-1} c_k(t) \text{Tr}\{T_i [T_k, T_j]\}. \quad (\text{A4})$$

Considering the commutator and anticommutator of the  $\text{SU}(N)$  generators,

$$[T_k, T_j] = i \sum_{m=1}^{N^2-1} f_{kjm} T_m, \quad (\text{A5})$$

$$\{T_k, T_j\} = \frac{\delta_{kj}}{N} I + \sum_{m=1}^{N^2-1} d_{kjm} T_m, \quad (\text{A6})$$

we obtain the coherent part in the Liouvillian supermatrix,

$$\mathcal{C}_{ij} = \sum_{k=1}^{N^2-1} \sum_{m=1}^{N^2-1} f_{kjm} c_k(t) \text{Tr}\{T_i T_m\} = \sum_{k=1}^{N^2-1} \frac{f_{kji}}{2} c_k(t), \quad (\text{A7})$$

where  $f_{ijk}$  and  $d_{ijk}$  are the structure constants and the  $d$  coefficients of the  $\text{SU}(N)$  Lie algebra, respectively.

The incoherent part can be expressed as

$$\mathcal{I}_{ij} = \text{Tr} \left[ T_i^\dagger \sum_{\alpha} \gamma_{\alpha} (2L_{\alpha} T_j L_{\alpha}^\dagger - \{L_{\alpha}^\dagger L_{\alpha}, T_j\}) \right]. \quad (\text{A8})$$

The Lindblad operators can also be expanded by the  $\text{SU}(N)$  Hermitian generators  $\{T_i\}_{i=1}^{N^2-1}$ , i.e.,

$$L_{\alpha}(t) = \sum_{j=1}^{N^2-1} l_j^{(\alpha)}(t) T_j, \quad (\text{A9})$$

with complex coefficients  $l_j^{(\alpha)}(t)$ , and

$$L_{\alpha}^{\dagger}(t) = \sum_{j=1}^{N^2-1} l_j^{(\alpha)*}(t) T_j, \\ L_{\alpha}^{\dagger}(t) L_{\alpha}(t) = \sum_{i=0}^{N^2-1} e_k^{(\alpha)}(t) T_k, \quad (\text{A10})$$

with  $e_n^{(\alpha)} = \frac{1}{2} \sum_{i,j=0}^{N^2-1} l_i^{(\alpha)}(t) l_j^{(\alpha)*}(t) (i f_{ijn} + d_{ijn})$  for  $n \neq 0$  and  $e_0^{(\alpha)} = \sum_{i=0}^{N^2-1} \frac{|l_i^{(\alpha)}(t)|^2}{2N}$ . Thus, it is easy to obtain

$$\text{Tr}[T_i^{\dagger} \{L_{\alpha}^{\dagger} L_{\alpha}, T_j\}] = e_0^{(\alpha)} \delta_{ij} + \sum_{k=1}^{N^2-1} \frac{d_{kji}}{2} e_k^{(\alpha)}, \\ \text{Tr}[T_i^{\dagger} L_{\alpha} T_j L_{\alpha}^{\dagger}] = \frac{l_i^{(\alpha)} l_j^{(\alpha)*}}{4N} + h_{ji}^{(\alpha)}, \quad (\text{A11})$$

with

$$h_{ji}^{(\alpha)} = \frac{1}{8} \sum_{p=1}^{N^2-1} \sum_{m,n=0}^{N^2-1} l_m^{(\alpha)} l_n^{(\alpha)*} (i f_{jnp} + d_{jnp}) (i f_{imp} + d_{imp}).$$

Rearranging the equations, we finally obtain the incoherent part of the Liouvillian supermatrix,

$$\mathcal{I}_{ij} = \sum_{m,n=0}^{N^2-1} \left( \sum_{\alpha} \gamma_{\alpha} l_m^{(\alpha)}(t) l_n^{(\alpha)*}(t) \right) s_{mn,ji}, \quad (\text{A12})$$

with

$$s_{mn,ji} = \frac{1}{2N} (\delta_{im} \delta_{jn} - \delta_{mn} \delta_{ij}) \\ + \frac{1}{4} \sum_{k=1}^{N^2-1} ((i f_{jnk} + d_{jnk}) (i f_{imk} + d_{imk}) \\ - (i f_{mnk} + d_{mnk}) d_{kji}), \quad (\text{A13})$$

where  $|l_m^{(\alpha)}(t)|^2 = \sum_n l_m^{(\alpha)}(t) l_n^{(\alpha)*}(t) \delta_{mn}$  has been used.

The last term in Eq. (A1) originates from the expansion of  $\mathcal{L}$  with the basis  $|T_i\rangle\rangle\langle\langle T_0|$ . For  $j = 0$ , this term can be written as

$$\mathcal{L}_k^0(t) = 2\text{Tr} \left\{ T_k^{\dagger} \sum_{\alpha} \gamma_{\alpha} (t) [L_{\alpha}(t) L_{\alpha}^{\dagger}(t) - L_{\alpha}^{\dagger}(t) L_{\alpha}(t)] \right\} \\ = \sum_{\alpha} \gamma_{\alpha}(t) \left\{ \sum_{i,j=1}^{N^2-1} l_i^{(\alpha)}(t) l_j^{(\alpha)*}(t) \right. \\ \left. \times [(i f_{jik} + d_{jik}) - (i f_{ijk} + d_{ijk})] \right\}. \quad (\text{A14})$$

**APPENDIX B: CONTROL PROTOCOL WITHOUT  $\Omega_y^R$** 

We also consider the two-level system used in Sec. III, whose dynamics is governed by the non-Markovian master

equation (17). Here we consider the renormalized control field to be real, and there is a detuning  $\Delta^R$  to the two-level system. Thus, the Hamiltonian in Eq. (17) can be written as

$$H_s^R(t) = s_0(t)\sigma_+\sigma_- + \Delta^R(t)\sigma_z + \Omega_x^R(t)\sigma_x. \quad (\text{B1})$$

We still assume that the spectrum density is untunable in experimental settings. At this time, the coherent control parameters are  $\Omega_x^R(t)$  and  $\Delta^R(t)$ , while the main excited number  $N(t)$  acts as the incoherent control parameter. Inserting the control parameters and the components of the Bloch vector into Eq. (13) yields

$$\begin{aligned} \dot{r}_x &= -(s_0 + \Delta^R)r_y - (2N + 1)\Gamma_0 r_x, \\ \dot{r}_y &= (s_0 + \Delta^R)r_x - (2N + 1)\Gamma_0 r_y, \\ \dot{r}_z &= 2\Omega_x^R r_y - 2\Gamma_0[(2N + 1)r_z + 1]. \end{aligned} \quad (\text{B2})$$

We can reverse solve Eq. (B2) and obtain

$$\begin{aligned} \Omega_x^R &= \frac{(2\Gamma_0 + \partial_t r_z)(r_x^2 + r_y^2) - \partial_t(r_x^2 + r_y^2)r_z}{2r_y(r^2 + r_z^2)}, \\ \Delta^R &= -s_0 + \frac{r_x(r_y\dot{r}_y + r_z\dot{r}_z) + 2\Gamma_0 r_x r_z - \dot{r}_x(r_y^2 + 2r_z^2)}{r_y(r_x^2 + r_y^2 + 2r_z^2)}, \\ N &= -\frac{2\Gamma_0 r_z + \vec{r} \cdot \dot{\vec{r}} + \Gamma_0(r^2 + r_z^2)}{2\Gamma_0(r^2 + r_z^2)}. \end{aligned} \quad (\text{B3})$$

Thus, we obtain a control protocol without  $\Omega_y^R$ . This protocol has advantages in the population-reversion task because the singular points of the control parameters appear only at  $r_y = 0$ . We may design the trajectory of the quantum state away from points with  $r_y = 0$ . For the complete population reversion, the initial and final states require  $r_y = 0$ . However, we can set proper boundary conditions for  $r_i$  and  $\dot{r}_i$  to eliminate those singular points.

- 
- [1] C. P. Koch, M. Lemeshko, and D. Sugny, *Rev. Mod. Phys.* **91**, 035005 (2019).
- [2] S. Osnaghi, P. Bertet, A. Auffeves, P. Maioli, M. Brune, J. M. Raimond, and S. Haroche, *Phys. Rev. Lett.* **87**, 037902 (2001).
- [3] S. Hacoheh-Gourgy, L. P. García-Pintos, L. S. Martin, J. Dressel, and I. Siddiqi, *Phys. Rev. Lett.* **120**, 020505 (2018).
- [4] L. C. Venuti, T. Albash, M. Marvian, D. Lidar, and P. Zanardi, *Phys. Rev. A* **95**, 042302 (2017).
- [5] R. Dann, A. Tobalina, and R. Kosloff, *Phys. Rev. Lett.* **122**, 250402 (2019).
- [6] S. Zippilli and D. Vitali, *Phys. Rev. Lett.* **126**, 020402 (2021).
- [7] R. H. Zheng, Y. Xiao, S. L. Su, Y. H. Chen, Z. C. Shi, J. Song, Y. Xia, and S. B. Zheng, *Phys. Rev. A* **103**, 052402 (2021).
- [8] S. L. Wu, W. Ma, X. L. Huang, and X. X. Yi, *Phys. Rev. Appl.* **16**, 044028 (2021).
- [9] F. Liu, X. Zhou, and Z. W. Zhou, *Phys. Rev. A* **99**, 052119 (2019).
- [10] W.-M. Zhang, P.-Y. Lo, H.-N. Xiong, M. W.-Y. Tu, and F. Nori, *Phys. Rev. Lett.* **109**, 170402 (2012).
- [11] L. Li, M. J. Hall, and H. M. Wiseman, *Phys. Rep.* **759**, 1 (2018).
- [12] G. Gasbarri and L. Ferioldi, *Phys. Rev. A* **97**, 022114 (2018).
- [13] M. R. Jørgensen and F. A. Pollock, *Phys. Rev. A* **102**, 052206 (2020).
- [14] I. de Vega and D. Alonso, *Rev. Mod. Phys.* **89**, 015001 (2017).
- [15] A. Pereverzev and E. R. Bittner, *J. Chem. Phys.* **125**, 104906 (2006).
- [16] F. Minganti, A. Biella, N. Bartolo, and C. Ciuti, *Phys. Rev. A* **98**, 042118 (2018).
- [17] D. Basilewitsch, F. Cosco, N. L. Gullo, M. Möttönen, T. Ala-Nissilä, C. P. Koch, and S. Maniscalco, *New J. Phys.* **21**, 093054 (2019).
- [18] A. Shabani and H. Neven, *Phys. Rev. A* **94**, 052301 (2016).
- [19] K. Seetharam, A. Leroose, R. Fazio, and J. Marino, *arXiv:2101.06445*.
- [20] A. Pechen and H. Rabitz, *Phys. Rev. A* **73**, 062102 (2006).
- [21] S. Alipour, A. Chenu, A. T. Rezakhani, and A. del Campo, *Quantum* **4**, 336 (2020).
- [22] X. Chen, I. Lizuain, A. Ruschhaupt, D. Guéry-Odelin, and J. G. Muga, *Phys. Rev. Lett.* **105**, 123003 (2010).
- [23] R. Wu, A. Pechen, C. Brif, and H. Rabitz, *J. Phys. A* **40**, 5681 (2007).
- [24] A. Grigoriu, H. Rabitz, and G. Turinici, *J. Math. Chem.* **51**, 1548 (2013).
- [25] M. Lostaglio, K. Korzekwa, and A. Milne, *Phys. Rev. A* **96**, 032109 (2017).
- [26] B. Buča and T. Prosen, *New J. Phys.* **14**, 073007 (2012).
- [27] H. Z. Shen, M. Qin, X. M. Xiu, and X. X. Yi, *Phys. Rev. A* **89**, 062113 (2014).
- [28] W. Cui, Z. R. Xi, and Y. Pan, *Phys. Rev. A* **77**, 032117 (2008).
- [29] H. Z. Shen, M. Qin, and X. X. Yi, *Phys. Rev. A* **88**, 033835 (2013).
- [30] P. Haikka and S. Maniscalco, *Phys. Rev. A* **81**, 052103 (2010).
- [31] D. Ran, W. J. Shan, Z. C. Shi, Z. B. Yang, J. Song, and Y. Xia, *Phys. Rev. A* **101**, 023822 (2020).
- [32] K. Hornberger, *Phys. Rev. Lett.* **97**, 060601 (2006).
- [33] C. P. Koch, *J. Phys.: Condens. Matter* **28**, 213001 (2016).
- [34] S. L. Wu, X. L. Huang, and X. X. Yi, *Phys. Rev. A* **99**, 042115 (2019).
- [35] V. Cavina, A. Mari, and V. Giovannetti, *Phys. Rev. Lett.* **119**, 050601 (2017).
- [36] J. Anders and M. Esposito, *New J. Phys.* **19**, 21 (2017).
- [37] H. J. D. Miller, M. H. Mohammady, M. Perarnau-Llobet, and G. Guarnieri, *Phys. Rev. Lett.* **126**, 210603 (2021).
- [38] S. H. Raja, S. Maniscalco, G. S. Paroanu, J. P. Pekola, and N. L. Gullo, *New J. Phys.* **23**, 033034 (2021).
- [39] Y. H. Kang, Z. C. Shi, B. H. Huang, J. Song, and Y. Xia, *Phys. Rev. A* **101**, 032322 (2020).
- [40] Z. C. Shi, C. Zhang, L. T. Shen, Y. Xia, X. X. Yi, and S. B. Zheng, *Phys. Rev. A* **101**, 042314 (2020).
- [41] S. L. Wu, *Phys. Rev. A* **91**, 032104 (2015).
- [42] R. H. Zheng, Y. H. Kang, S. L. Su, J. Song, and Y. Xia, *Phys. Rev. A* **102**, 012609 (2020).
- [43] I. Medina and F. L. Semiao, *Phys. Rev. A* **100**, 012103 (2019).
- [44] B. Bylicka, M. Johansson, and A. Acín, *Phys. Rev. Lett.* **118**, 120501 (2017).
- [45] G. Guarnieri, C. Uchiyama, and B. Vacchini, *Phys. Rev. A* **93**, 012118 (2016).
- [46] S. G. Schirmer and X. Wang, *Phys. Rev. A* **81**, 062306 (2010).